

## Article

# Mercerization of Agricultural Waste: Sweet Clover, Buckwheat, and Rapeseed Straws

Madara Žiganova , Agnese Ābele , Zanda Iesalniece and Remo Merijs Meri

Institute of Polymer Materials, Faculty of Materials Science and Applied Chemistry, Riga Technical University, LV-1048 Riga, Latvia

\* Correspondence: madara.ziganova@rtu.lv

**Abstract:** This research presents the alkali treatment effect on three types of agricultural residues: sweet clover (SCS), buckwheat (BS), and rapeseed straws (RS). The aim of the study was to find the optimal treatment conditions for each straw type, and to assess the potential of sweet clover straw as reinforcement for polymer composites in comparison to buckwheat and rapeseed. The straws were ground and treated for 15, 30, and 60 min using NaOH at concentrations of 2, 5, and 10%. To investigate the treatment results on the SCS, BS, and RS fibers, Fourier transform infrared spectroscopy, scanning electron microscopy, optical microscope, X-ray diffraction, and thermogravimetric analysis were used. Results indicate that the optimal room-temperature alkaline-treatment conditions of SCS fibers were the same as those for RS treated with 2% NaOH solution for 30 min. These conditions were milder in comparison to those used for the treatment of BS: 60 min in a 5% NaOH solution. During the treatment, noncellulosic substances were largely removed, and the aspect ratio of the fibers was increased, and the destruction temperature, crystallinity, and morphology were also affected. Consequently, SCS has promising potential for use in polymer composites.

**Keywords:** sweet clover fibers; rapeseed fibers; buckwheat fibers; alkali treatment; lignocellulosic biomass



**Citation:** Žiganova, M.; Ābele, A.; Iesalniece, Z.; Meri, R.M.

Mercerization of Agricultural Waste: Sweet Clover, Buckwheat, and Rapeseed Straws. *Fibers* **2022**, *10*, 83. <https://doi.org/10.3390/fib1010083>

Academic Editor: Carlo Santulli

Received: 24 August 2022

Accepted: 23 September 2022

Published: 28 September 2022

**Publisher's Note:** MDPI stays neutral with regard to jurisdictional claims in published maps and institutional affiliations.



**Copyright:** © 2022 by the authors. Licensee MDPI, Basel, Switzerland. This article is an open access article distributed under the terms and conditions of the Creative Commons Attribution (CC BY) license (<https://creativecommons.org/licenses/by/4.0/>).

## 1. Introduction

Researchers with different backgrounds and objectives have spent decades studying the valorization of lignocellulosic biomass waste. One of the fields where this renewable material source still has growing interest is the development of polymer composites. A fiber obtained from lignocellulosic biomass has several advantages, for example, low cost, biodegradability, availability, and relatively high specific strength, which allow for its use for the replacement of synthetic fibers. Various plants have been investigated for the production of natural fibers considering aspects such as global production, local availability, and chemical composition because higher cellulose content could provide better strength properties. However, there are only few investigations related to use of agricultural residues, such as rapeseed (RS), buckwheat (BS), and especially sweet clover (SCS) straws, for the production of fibers for bulk polymer composites. Fewer studies related to SCS evidently connected production amounts with it. For example, in Latvia, sown areas of rapeseed alone reach 117.4 tons per hectare (t/ha), 20.3 t/ha for buckwheat, and only 1.5 t/ha for sweet clover [1]. Furthermore, because of the transformation of the linear economy into a circular one, it is necessary to identify all locally available renewable resources [2]. Apart from the primary use of rapeseed for oil production, buckwheat as a food nutrient, and sweet clover as a high-value nectar plant, residues of these crops are without high added value, and may be utilized as solid fuel, green manure, and fodder, to a limited extent because of their low feeding value and potential toxicity [3]. Especially problematic are residues from sweet clover due to the high content of coumarin, which is converted into dicoumarol by mold in hay and becomes dangerous for livestock [4].

Therefore, the search for alternative ways for the high added-value utilization of these agricultural residues is highly important.

The chemical composition of the fibers obtained from the mentioned agricultural residues differs to certain extent: RS contains approx. 33–42% cellulose, 29% lignin, and hemicellulose up to 25% [5]; SCS contains approx. 55% cellulose, 14% lignin, and 18% hemicellulose [4]; and BS contains approx. 42% cellulose, 17% lignin, and 9% hemicellulose [6]. By considering the reinforcing properties of cellulose, fibers from the selected agricultural residues have potential to be used in polymer composites.

Nevertheless, before the development of fiber-reinforced composites, fiber treatment should be performed. According to the review by Hasan et al., lignocellulosic fiber is characterized by high hydrophilicity due to noncellulose constituents that provide swelling, water absorption, and, at the composite development limit, interfacial adhesion with a hydrophobic polymer matrix. Researchers have investigated various physical and chemical treatment procedures to reduce or remove hemicellulose, lignin, pectin, wax, and other low-molecular-weight fractions for increasing the compatibility with polymers. There are several chemical treatment methods, including mercerization, acetylation, silane treatment, peroxide treatment, and benzylation [7]. A comparison between different treatment methods is complicated; each process has its advantages, as was reported by Sanjay et al. For example, isocyanate treatment significantly improves the mechanical properties of fiber, silane treatment improves the physicochemical properties, and acetic acid treatment improves the tensile properties and thermal stability [8].

One of the most frequently used methods is alkali treatment (mercerization), which helps in removing unwanted substances by reducing the hydroxyl group concentration on the fiber surface, decreasing the fiber diameter, increasing the aspect ratio and surface roughness, providing better interlocking with the matrix, and ensuring cost efficiency in comparison to other fiber treatment methods. During mercerization, fibers swell, and in this process, part of the hydrogen bonds are destroyed, and a new Na-cellulose lattice is formed. In the consequent washing stage, Na ions and surface impurities are removed. Treatment efficiency is generally determined via temperature, time, and alkali concentration [7,8]. According to the review by Hasan et al., it follows that a too-high alkali concentration or temperature could lead to a significant decrement in fiber properties due to excessive delignification [7].

By considering the previously mentioned, this research focused on evaluating the valorization potential of RS, BSF, and especially SCS biomass for reinforcement in polymer composites. The study aims to find the optimal alkali solution concentration and process time for the treatment of each straw type (RS, BSF, SCS). Experiments were conducted to evaluate the effect of mercerization on the structure, chemical composition, and thermal properties of the fibers for the potential use of the treated fibers as reinforcement in polymer composites.

## 2. Materials and Methods

### 2.1. Materials

Winter rapeseed straw (RS), buckwheat straw (BS), and sweet clover straw (SCS) were collected as biomass waste from local farms Brasliņi, Pasiles, and Susuri. Sodium hydroxide pellets EMSURE were supplied by Sigma Aldrich. Straws were ground with a Retsch SM300 rotary grinder at a speed of 700 rpm using a 0.25 mm sieve. The fibers were dried in an oven for 24 h at 60 °C.

### 2.2. Fiber Alkali Treatment (Mercerization)

A certain amount (50 g) of the ground RS, BS, and SCS fibers was immersed in 3 different aqueous solutions with NaOH concentrations of 2%, 5%, and 10%, and each obtained suspension was mixed for 15, 30, and 60 min. At the end of mercerization, the fibers were washed several times using distilled water until neutral reaction. The treated fibers were dried in an oven at 60 °C for about 24 h.

### 2.3. Fiber Characterization

#### 2.3.1. Optical Microscopy (OM)

The length and diameter of the fibers were examined with optical microscope Leica DMRM. The images were processed with Fiji image analysis software. The mean diameter and mean length of RS, BS, and SCS fibers were determined from 50 measurements. The aspect ratio was correspondingly calculated.

#### 2.3.2. Scanning Electron Microscopy (SEM)

The surface morphologies of the fibers were analyzed with a Tescan Mira/LMU scanning electron microscope operated at 5 kV and 3000× magnification. The samples before morphology analysis were coated with gold layer using plasma sputtering apparatus Emitech/Quorum sputter coater K550X.

#### 2.3.3. X-ray Diffractometer (XRD)

X-ray diffraction patterns were recorded with a Panalytical Aeris Benchtop X-ray diffractometer at 2θ range from 5° to 40° with a step size of 0.0434° and a step time of 240 s. The crystallinity index (CI) of the fibers was calculated by using Segal's equation:

$$CI(\%) = \frac{I_{200} - I_{am}}{I_{200}} \times 100 \quad (1)$$

where  $I_{200}$  is an intensity of the (200) peak of crystalline cellulose (at a 2θ angle value between 20.0° and 22.3°), and  $I_{am}$  is the intensity of the amorphous cellulose fraction (at 2θ~18°).

#### 2.3.4. Fourier Transform Infrared Spectroscopy (FTIR)

FTIR spectra were obtained with a Thermo Fisher Scientific Nicolet 6700 spectrometer via the attenuated total reflectance (ATR) technique. All spectra were recorded in the range of 650 to 4000  $\text{cm}^{-1}$  with a resolution of 4  $\text{cm}^{-1}$ .

#### 2.3.5. Thermogravimetric Analysis (TGA)

Thermal properties were evaluated using thermogravimetric analyzer MettlerToledo TGA1/SF. About 10 mg of the test sample was heated under an air flow atmosphere from 25 to 600 °C with a heating rate of 10 °C/min.

#### 2.3.6. Chemical Composition Analysis

Untreated and treated straw characterization was carried out at the Latvian State Institute of Wood Chemistry according to the method described elsewhere [9].

## 3. Results and Discussion

### 3.1. FTIR

Figure 1 shows the FTIR spectra of the untreated BS, RS, and SCS fibers. The spectra were typical to lignocellulosic materials with slight differences due to variations in the chemical composition (see Table 2). Lignocellulose material has a complicated structure that is affected by cellulose, hemicellulose, and lignin, and other compounds such as wax and pectin [8,10]. The maxima of the most significant FTIR peaks of the investigated SCS, BS, and RS fibers are shown in Table 1.

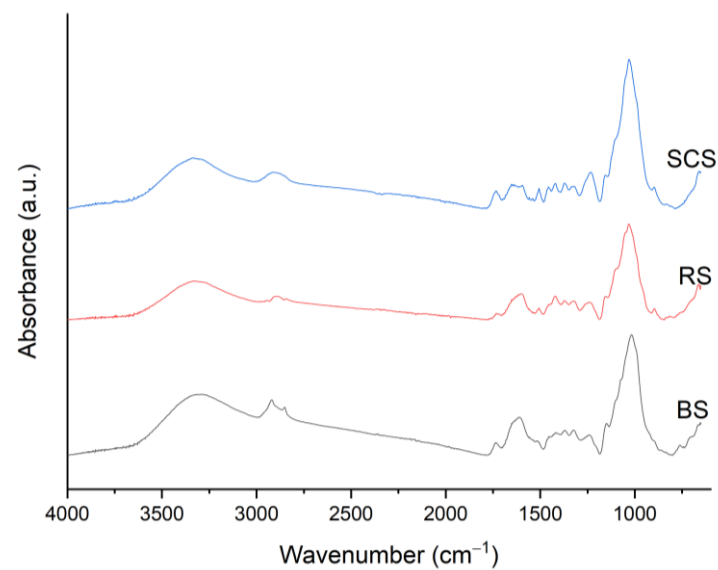
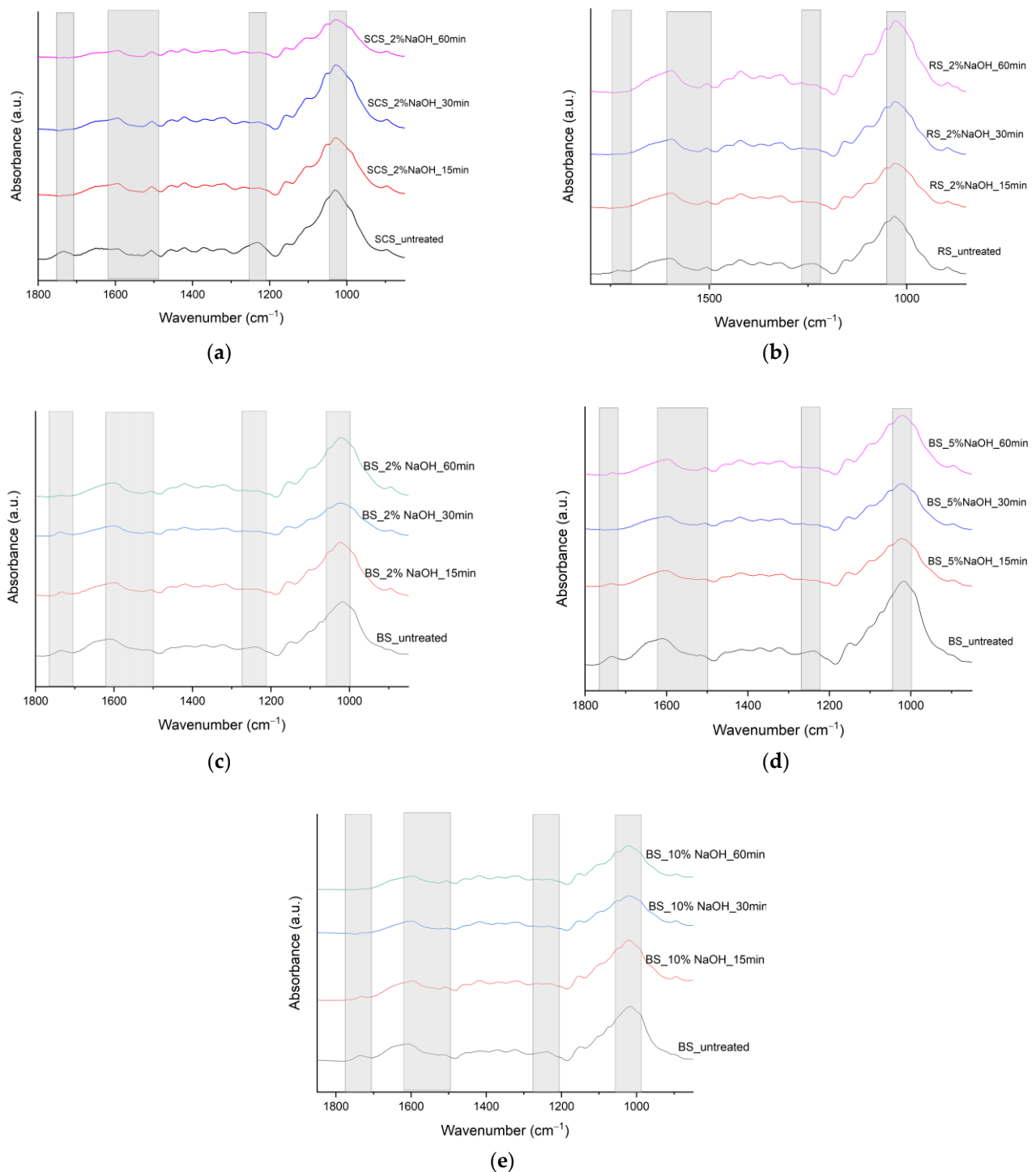


Figure 1. FTIR spectra of untreated BS, RS, and SCS fibers.

Table 1. FTIR peaks and corresponding functional groups of SCS, BS, and RS [11–13].

SCS $\nu$ ( $\text{cm}^{-1}$ )	BS $\nu$ ( $\text{cm}^{-1}$ )	RS $\nu$ ( $\text{cm}^{-1}$ )	Peak Assignment	References
3328	3283	3322	O–H stretching vibration in cellulose	[11–13]
2912	2918 and 2855	2891	C–H stretching vibrations of methyl and methylene groups in cellulose, hemicellulose, pectin, and fatty acids and lipids	[11–13]
1733	1732	1732	Carboxyl/aldehyde group in hemicellulose; carbonyl/carboxyl groups in lignin, pectin, or waxy fraction	[11–13]
1652	1614	1598	C=C double bonds in aromatic moieties in lignin; may overlap with OH bending of water	[11,12]
1506	1506	1506	C=C stretching in lignin	[5]
1418	1416	1418	CH <sub>2</sub> bending in cellulose	[13]
1373	1370	1372	C–H bending in cellulose and hemicellulose	[11]
1319	1324	1319	CH <sub>2</sub> wagging in crystalline cellulose	[11]
1234	1241	1235	C–O stretching of hemicellulose or C–O–C of lignin	[11–13]
1030	1018	1031	C–O stretching of cellulose and C–H deformation in lignin	[11,12]
898	–	896	C–O–C and C–H out-of-plane bending or stretching in amorphous cellulose; $\beta$ -glycosidic linkages of cellulose	[11–13]

Although the absorbance bands of different lignocellulose components overlap, after alkali treatment, some common trends were observed for BS, RS and SCS. As shown in Figure 2, the peak at  $1730\text{ cm}^{-1}$  disappeared after increasing alkali treatment time due to the removal of low-molecular-weight compounds [11]. Comparatively, the removal of noncellulosic impurities was the slowest in the case of BS, i.e., the treatment with a 2% alkali solution (Figure 2c) was not as efficient as the treatment with a higher concentration of alkali (Figure 2d). At the same time, the disappearance of the peak was centered at  $1240\text{ cm}^{-1}$ , and the reduction in the peaks within a broad region between  $1652$  and  $1500\text{ cm}^{-1}$ , and at  $1100\text{ cm}^{-1}$  shows that there was decreasing lignin and hemicellulose content. Consequently, FTIR results show that the chosen alkali treatment conditions (time, concentration) did not completely remove all lignin and hemicellulose.



**Figure 2.** FTIR spectra of untreated and treated (a) SCS, (b) RS, and (c–e) BS fibers.

According to the spectra, the peak for the hydroxyl (–OH) groups at  $\sim 3300\text{ cm}^{-1}$  wavenumber was the highest in fibers treated for 30 min. This was expected due to some of the lignin being removed. After lignin had been removed, the exposure of hydroxyl groups in hemicellulose and cellulose increased. The intensity of the hydroxyl groups eventually decreased with longer alkali treatment times. Results show that the hydroxyl stretching vibration continued to decrease as the treatment time increased to 16 h, which was expected due to the increased degradation of hemicellulose. After 16 h of treatment, very few changes were observed for the –OH peak. Since cellulose is fairly resistant to alkali

solutions, the minimal activity taking place during this time was possibly an indication that mostly cellulose was present on the surface.

### 3.2. Optical Microscopy

To determine the effect of alkali treatment on the length (L) and diameter (d) of the fiber, optical microscopy was conducted. According to Gomes et al., the fiber diameter decreases after treatment with NaOH because of the change in surface morphology. Analyzing SEM images, they concluded that the raw fiber was a bundle of monofilaments bonded by lignin and, because the alkali treatment removed a great amount of lignin, the fiber diameter was reduced [14]. In the current research, all the fibers showed a decrease in diameter after alkali treatment; Figure 3a shows where the highest decrement was observed for BS (48%), followed by that for SCS (46%) and RS (43%). The mean value of the fiber diameter is commonly reduced by increasing the concentration of the alkali solution and treatment time. However, in the current research, such a decrease in fiber diameter was not unambiguously observed. Such an observation could be explained by the surface relief development, and intracrystalline and interfibrillar swelling [15]. At the same time, alkali treatment changes and the aspect ratio can be seen in Figure 3b. The highest aspect ratio value for RS fibers was 12, obtained after the treatment with a 2% NaOH solution for 30 min. For SCS fibers, the highest aspect ratio was 5, obtained after treatment at different conditions. For BS fibers, the highest aspect ratio of 9 was reached after treatment with a 5% NaOH solution for 60 min.

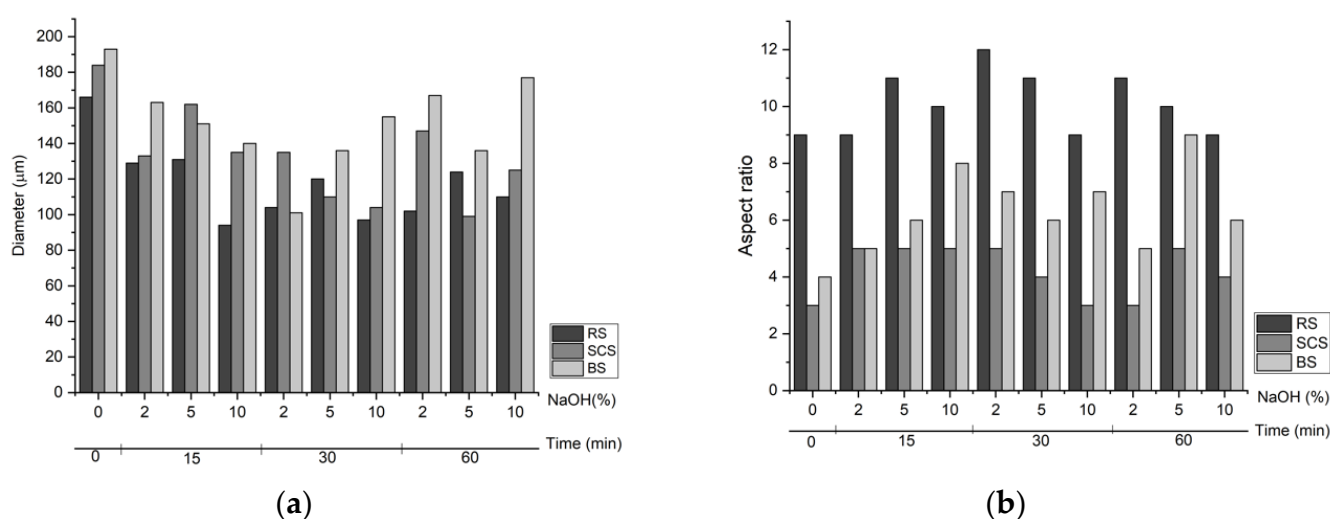


**Figure 3.** (a,b) Diameter aspect ratio of untreated and treated RS, SCS, and BS fibers.

In this research, the aspect ratio was considered to be one of the main indicators to determine the optimal treatment conditions for the fibers. However, by considering that, in the SCS fiber case, several treatments demonstrated almost identical results, thermal analysis was performed to evaluate the change in the thermal stability of the fibers after alkaline treatment.

### 3.3. Thermal Properties

TGA thermograms of SCS, RS and BS untreated and treated with 2%NaOH at different times are reported in Supplementary Information S1–S3. Considering that, during treatment with NaOH, the fiber surface was cleaned from noncellulose substances, this affected the thermal properties of the fibers and the residue amount. As shown in Figure 4, all three fibers showed a similar thermal degradation trend, demonstrating three thermal decomposition steps, as was also stated in the literature [16,17]. The first thermal degradation step, observed in the range from 25 to ~130 °C, demonstrates mass loss of 4.4%, 5.8%, and 6.3% for the untreated RS, SCS, and BS, respectively. The peak maxima were observed at

73 °C for BS, 84 °C for RS, and 87 °C for SCS, primarily indicating the release of moisture, although in this stage, the evaporation of low-molecular-weight compounds (extractives) might also occur [16]. After the treatment decrement in mass loss had been observed, RS and SCS fibers lost approximately 3.6% from their initial mass, and BS fiber negligibly more, 4%, because the mercerization of fibers decreases water absorption [7]. Additionally, the peak maximum changed within a couple of degrees (in the SCS and RS fiber cases) or shifted towards higher temperature values (in the BS fiber case). For example, in the case of BS fibers treated with 5% NaOH solution for 30 min, the peak occurred at 95 °C.

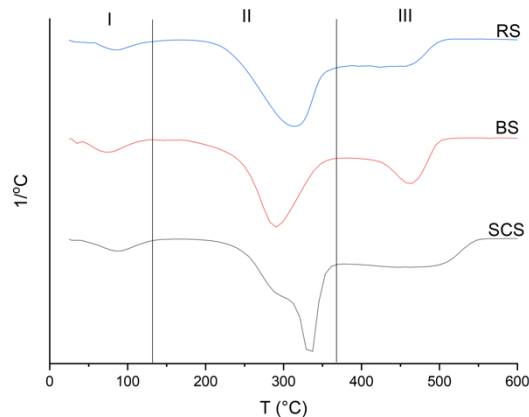


**Figure 4.** DTA curves of untreated RS, BS, and SCS fibers.

In the second segment, the thermal destruction of hemicellulose and cellulose moieties was observed. Hemicellulose degrades before cellulose due to its random amorphous structure. In the current study, its degradation temperature could not be clearly determined because of the overlap with cellulose degradation [17]; only in the SCS fiber case was a hemicellulose shoulder at 289 °C observed. Meanwhile, the major degradation peak of untreated BS, RS, and SCS fibers was observed at 290, 314, and 334 °C, respectively, corresponding to mass losses of 60%, 61%, and 55%. Figure 5 shows main degradation temperature ( $T_d$ ) within the second segment for all the investigated fibers. The highest increment of  $T_d$  was observed in the BS fiber case;  $T_d$  changed from 290 to 310 °C, most probably due to the more efficient removal of the hemicellulose fraction and extractives [17]. For SCS fibers, in contrast, a significant decrease in  $T_d$  was observed, i.e., the  $T_d$  of the treated fibers decreased from 334 to 304–311 °C. This may be explained by the less efficient removal of hemicellulose fraction and its possible effect on the structure of crystalline cellulose during the treatment [17,18]. The highest value of  $T_d$  (311 °C) corresponds to the SCS fibers treated with a 2% NaOH solution for 30 min. For the treated RS fibers,  $T_d$  fluctuated in the range between 302 and 316 °C. Furthermore, by increasing the alkali concentration, the  $T_d$  value of RS fibers greatly decreased.

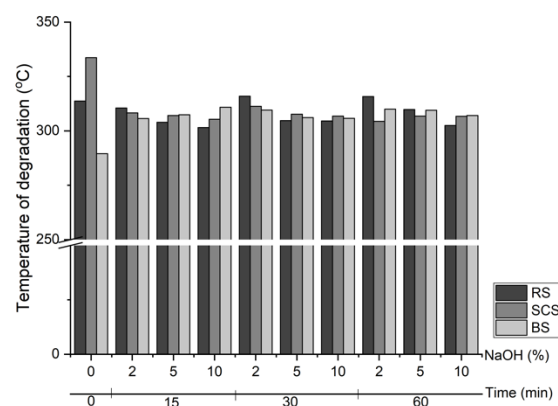


**Figure 5.** Second segment destruction temperature of untreated and treated RS, SCS, and BS fibers.

The third mass-loss stage is mostly attributed to lignin destruction. Lignin destruction occurs in a wide range from 250 to 600 °C [17]. Figure 4 demonstrates that, in the current investigation, the decomposition of the lignin phase within RS and SCS took place in a broader range than that in BS; this depends on the chemical structure of lignin, which is different for each of the investigated plant species. Lignin has very complex structure, and various oxygen functional groups or fractions have different thermal stability. According to Ando et al., higher thermal stability is associated with the presence of condensed lignin with a  $\beta$ -5 substructure [19].

Regarding residual mass (RM), untreated SCS fibers were characterized with the lowest value (4.4%) out of the three fibers. Overall, RM at 600 °C was decreased after alkaline treatment due to the removal of hemicellulose and lignin from the treated straw biomass. For example, after treatment with a 5% NaOH solution for 60 min, RM decreased from 4.4% to 3.4% for SCS, from 6.6% to 2.1% for RS, and from 6.2% to 3% for BS. The higher RM values were most probably due to the higher remaining lignin content in the fibers because of the more intense development of char [20].

From the results of TGA, optimal NaOH treatment conditions for the investigated fibers could be suggested by considering that the highest  $T_d$  and the lowest RM values were reached. Consequently, treatment with a 2% alkali solution for 30 min is suggested for RS and SCS fibers; for BS fibers, at least three different treatments options could be compared, namely, treatment with a 2% alkali solution for 30 min, treatment with a 5% alkali solution for 60 min, and treatment with a 10% alkali solution for 15 min. However, taking into consideration the results of FTIR measurements and the aspect ratio, the treatment of BS fibers with 5% NaOH for 60 min was suggested to be optimal.

### 3.4. Chemical Composition

Changes in the chemical composition of the untreated and the selected alkali-treated fibers are demonstrated in Table 2. These results indicate that, after treatment, the cellulose content insignificantly increased from 38 to 39% in BS, from 34 to 38% in SCS, and from 34 to 36% in RS. As it was expected, the selected treatment method mainly affected the hemicellulose fraction. Hemicellulose content changed most significantly, especially in the BS case, where it dropped about 33%, in comparison to 30% for RS, and 21% for SCS. The acid-insoluble lignin fraction changed insignificantly. However, during chemical composition analysis, not all compounds were identified. Among unidentified compounds, there are waxes, extractives, pectin, and acid-soluble lignin [10]. This may influence the total lignin content in the fibers before and after alkali treatment.

**Table 2.** Chemical compositions of untreated and treated BS, SCS, and RS fibers.

Compound	Fiber			Fiber after Optimal Treatment		
	BS	SCS	RS	BS_5%NaOH _60 Min	SCS_2%NaOH _30 Min	RS_2%NaOH _30 Min
Amount % from Dry Mass						
Glucose	42.43	37.48	37.67	43.58	42.52	39.70
Xylose	9.82	14.66	17.36	8.36	13.75	14.81
Galactose	2.42	1.34	1.68	1.26	1.18	1.30
Arabinose	0.51	0.83	1.36	0.79	0.56	0.72
Mannose	1.18	2.04	2.95	1.49	2.10	2.30
Acetic acid	3.94	4.18	3.94	0.00	0.28	0.18
Levulinic acid, formic acid, 5-HMF	1.43	0.98	1.43	1.02	1.17	1
Ash	0.05	3.02	0.06	0.02	3.41	0.02
Insoluble lignin	18.7	25.76	21.75	19.27	23.81	21.22

### 3.5. Surface Morphology

Alkali treatment also influences the fiber morphology; some of the untreated and treated fibers SEM images are presented in Figure 6. On the external surfaces of the investigated fibers, different types of impurities, such as waxes, extractives and tyloses (fatty deposits) were observed [16]. During mercerization (1), alkali reacts with fiber hydroxyl groups, (2) lignin, hemicellulose, and other impurities are removed, (3) fiber cell walls are affected, and (4) fiber bundles are broken, resulting in increased purity and surface roughness (Figure 6b,d,f) [7,21]. After alkali treatment, the surface of SCS fibers (Figure 6d) is characterized with expressed globular marks, which could show the presence of tyloses; in comparison with BS and RS fibers, it looks rougher. SEM observation of the fiber surfaces after alkali treatment showed regular, small pores or pits (with a diameter of about 1  $\mu\text{m}$  for RS, 1.2  $\mu\text{m}$  for SCS, and 1.4  $\mu\text{m}$  for BS fibers) that are channels for transporting water and nutrients for the plant. Pits for untreated fibers are invisible due to impurities and a layer of wax [16,22]. Consequently, the alkali treatment increased the surface accessibility (via opening pores, cracks) of the investigated fibers, which is important for obtaining polymer–fiber composites. This promotes better adhesion between components and allows for polymer interlocking in the fiber through pores and cracks, improving the mechanical bonding of fibers and polymers. Furthermore, by reducing the content of impurities, it is possible to decrease the hydrophilic character of fibers, which may also improve compatibility with a hydrophobic polymer matrix [23].

### 3.6. XRD

During alkali treatment, noncellulose substances are removed, and the cellulose crystalline structure is rearranged because cellulose hydrogen bonds and van der Waal's forces are broken [24]. As a result, XRD patterns of the investigated fibers are changed. Typical crystallographic planes for cellulose I are at  $2\theta = 14.5\text{--}15.3^\circ$  (1–10),  $15.7\text{--}16.8^\circ$  (110),  $21.9\text{--}22.6^\circ$  (200) and  $34^\circ$  (004), but at  $2\theta = 18.3\text{--}18.4^\circ$  [17,24,25] for the amorphous phase. The XRD patterns (Figure 7) of the investigated untreated lignocellulosic fibers showed peaks at  $2\theta = 16^\circ$ ,  $21.8^\circ$ ,  $26.1^\circ$ ,  $26.7^\circ$  and  $29.5^\circ$  for RS, at  $2\theta = 14.5^\circ$ ,  $16.8^\circ$ ,  $21^\circ$ ,  $21.8^\circ$ ,  $26.7^\circ$  and  $32.4^\circ$  for BS, and at  $2\theta = 15.7^\circ$ ,  $20.9^\circ$ ,  $22^\circ$  and  $26.7^\circ$  for SCS that were assigned to crystallographic planes and the amorphous phase, respectively. The diffraction peaks of all the treated fibers were more intense, especially at crystallographic plane 004. The main diffraction peak (200) was shifted to  $22.1^\circ$  for BS,  $22.3^\circ$  for SCS, and  $22.1^\circ$  for RS; in the SCS and BS cases, double peaks disappeared, and a single main peak was observed. At  $2\theta = \sim 16^\circ$ , a broad peak was observed; therefore, it was impossible to determine cellulose I crystalline forms (triclinic and monoclinic) due to the peaks overlapping. Furthermore, after alkaline treatment, the crystallinity index of the fibers increased from 43% to 48% for RS, from 37% to 47% for BS, and from 38% to 57% for SCS, the highest extent. However, crystallinity determined from XRD by using the Segal method (Equation (1)) represents partial crystallinity because it only considers the main peak of the 200 plane [17].

XRD can also indicate the conversion of cellulose I into cellulose II, which is a well-known transformation during mercerization. In the current research, results are not unambiguous because lignin and hemicellulose remained within the treated fibers and may have affected diffraction peaks due to their scattering halos overlapping with cellulose diffraction in the investigated range [26].

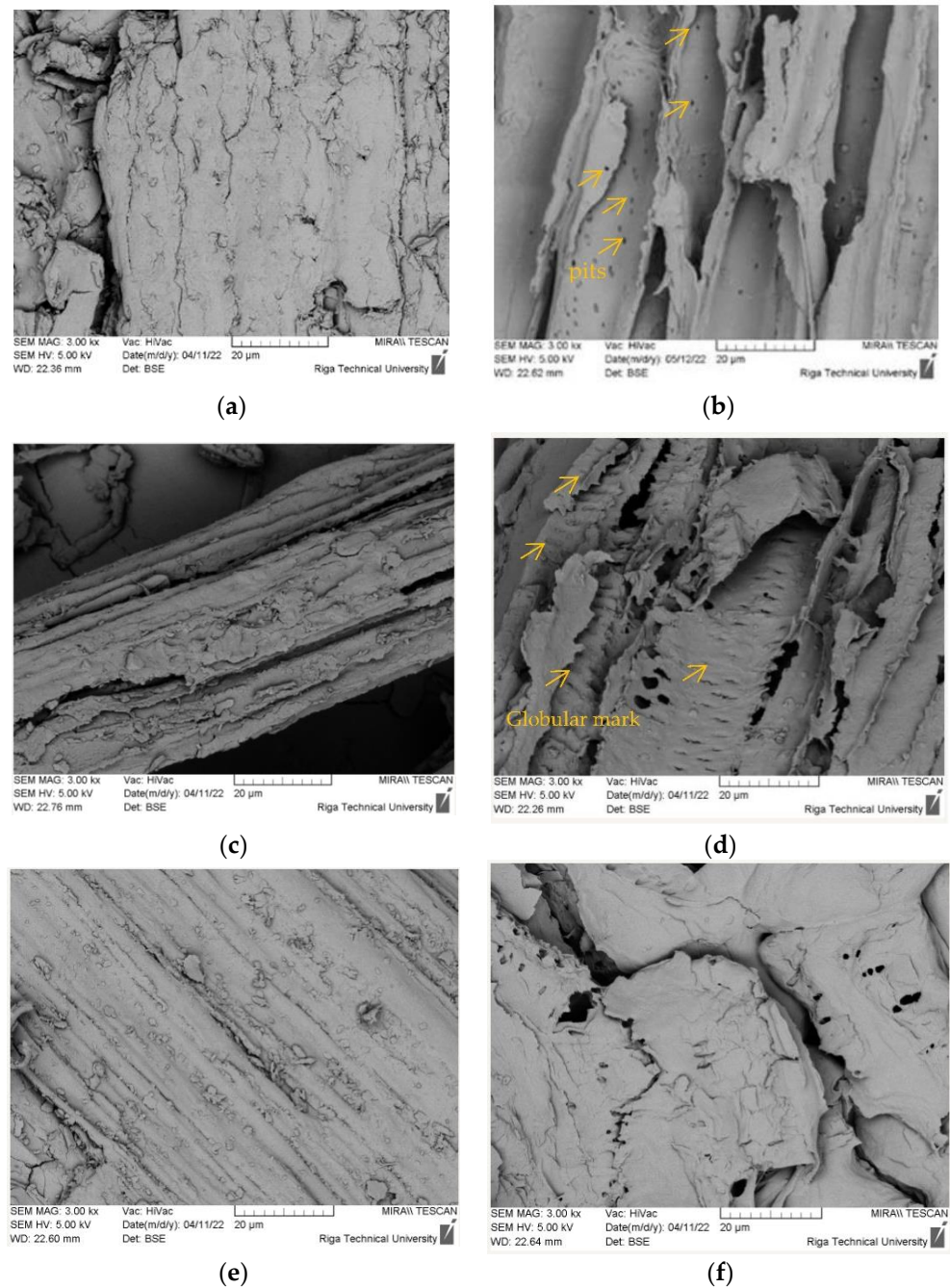


**Figure 6.** SEM surface images of (a,c,e) untreated and (b,d,f) treated (a,b) RS, (c,d) SCS, and (e,f) BS fibers at the suggested treatment conditions (i.e., with 2% NaOH solution for 30 min for SCS and RS fibers, and with 5% NaOH solution for 60 min for BS fibers).

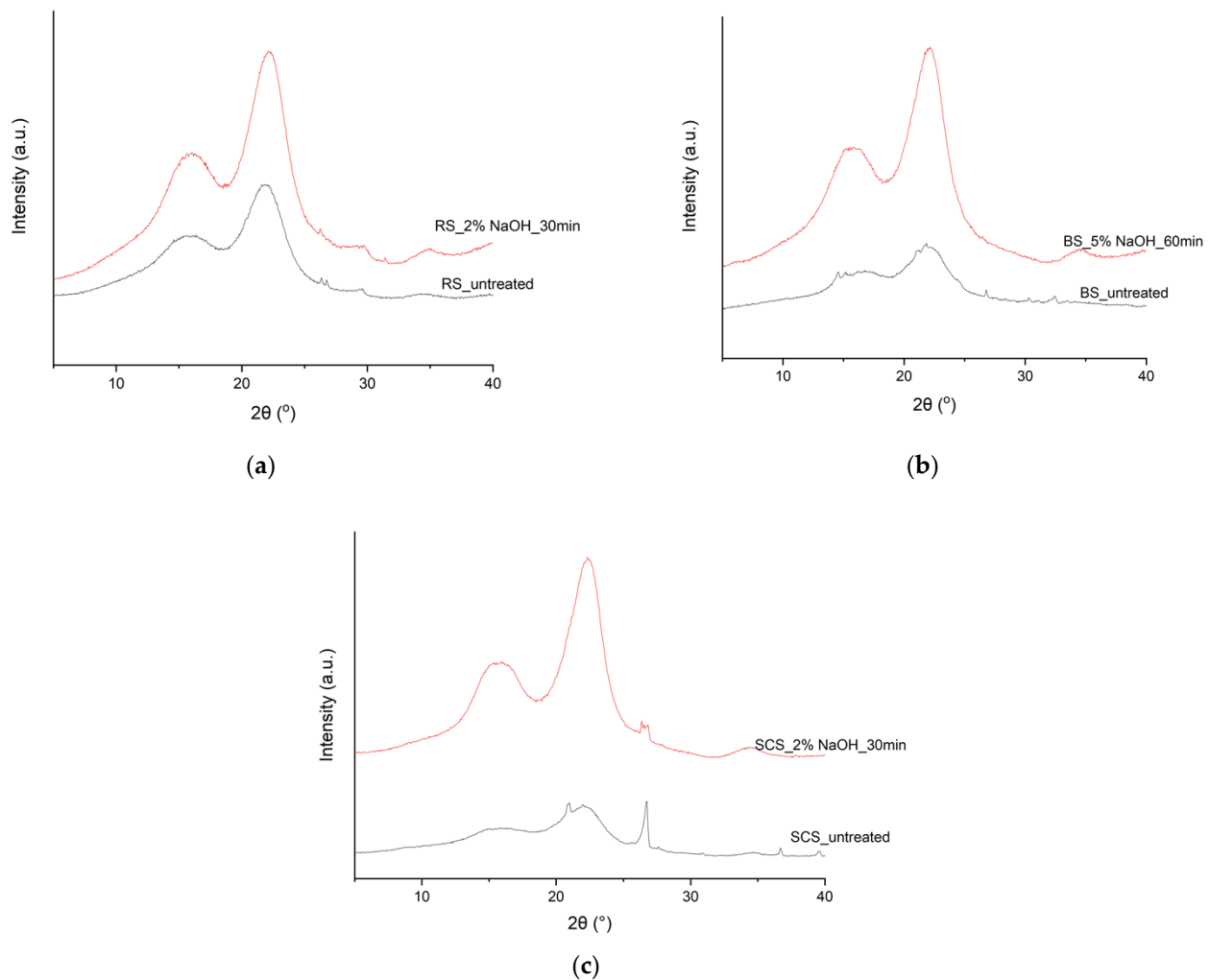


**Figure 7.** X-ray diffraction patterns of untreated and treated (a) RS, (b) BS, and (c) SCS fibers.

#### 4. Conclusions

This research showed that locally obtained agricultural residue biomass from BS, RS, and SCS is promising for the reinforcement of polymer composites. The intrinsic incompatibility of BS, RS, and SCS fibers with hydrophobic polymer matrices was successfully reduced via the mercerization process with the partial removal of noncellulose substances, confirmed via microscopy, FTIR, XRD, and TGA measurements. The increased crystallinity and improved thermal stability of the alkali-treated fibers, as determined by XRD and TGA, respectively, were considered to be additional factors determining the suitability of BS, RS, and SCS biomass as a potential alternative source for the production of reinforcing fibers for polymer composites. Optimal alkali treatment conditions (solution concentration and process time) at room temperature for each of the investigated fiber types were also found. In particular, the highest aspect ratio of RS (12) and SCS (5) fibers was found after room temperature treatment with a 2% NaOH solution for 30 min., whereas the highest aspect ratio for the BS (9) fiber was found at somewhat greater alkali concentrations (5%) and a longer treatment time (60 min).

**Supplementary Materials:** The following supporting information can be downloaded at: <https://www.mdpi.com/article/10.3390/fib10100083/s1>. Figure S1: TGA\_SCS\_2%\_all time; Figure S2: TGA\_RS\_2%\_all time; Figure S3: TGA\_BS\_2%\_all time.

**Author Contributions:** Conceptualization, A.Ā. and R.M.M.; methodology, Z.I.; investigation, M.Ž., Z.I. and A.Ā.; writing—original draft preparation, M.Ž., Z.I. and A.Ā.; writing—review and editing,

R.M.M.; funding acquisition, A.Ā. All authors have read and agreed to the published version of the manuscript.

**Funding:** This research was funded by The Latvian Science Council, grant number LZIP 2021/1-0347.

**Data Availability Statement:** Not applicable.

**Acknowledgments:** The authors wish to acknowledge to Rudolfs Cimdins Riga Biomaterials Innovations and Development Centre of RTU, Institute of General Chemical Engineering for SEM and XRD tests.

**Conflicts of Interest:** The authors declare no conflict of interest.

## References

- Pilvere, I. Central Statistical Bureau Republic of Latvia. Lauksaimniecības Attīstības Prognozēšana un Politikas Scenāriju Izstrāde Līdz 2050. *Gadam Projekta Atskaite*. **2021**, *21*, 1–165. Available online: [www.csb.gov.lv/lv/statistika/statistikas-temas/lauksaimnieciba/aukopiba/meklet-tema/2605-lauksaimniecibas-kulturu-sejumu-platibas-un](http://www.csb.gov.lv/lv/statistika/statistikas-temas/lauksaimnieciba/aukopiba/meklet-tema/2605-lauksaimniecibas-kulturu-sejumu-platibas-un) (accessed on 1 August 2022).
- European Parliament. Circular economy: Definition, Importance and Benefits. 2022. Available online: <https://www.europarl.europa.eu/news/en/headlines/economy/20151201STO05603/circular-economy-definition-importance-and-benefits> (accessed on 23 August 2022).
- Manitoba Government Inquiry, Extending Livestock Feed Supplies Section One. Available online: <https://www.gov.mb.ca/agriculture/livestock/production/beef/extending-livestock-feed-supplies-section-one.html#6> (accessed on 23 August 2022).
- Rigal, M.; Rigal, L.; Vilarem, G.; Vandebossche Maréchal, V. Sweet Clovers, a Source of Fibers Adapted for Growth on Wet and Saline Soils. *J. Nat. Fibers* **2016**, *13*, 410–422. [[CrossRef](#)]
- Brahim, M.; Boussetta, N.; Grimi, N.; Vorobiev, E.; Zieger-Devin, I.; Brosse, N. Pretreatment optimization from rapeseed straw and lignin characterization. *Ind. Crops Prod.* **2017**, *95*, 643–650. [[CrossRef](#)]
- Smuga-Kogut, M.; Bychto, L.; Walendzik, B.; Cielecka-Piontek, J.; Marecik, R.; Kobus-Cisowska, J.; Grajek, K.; Szymanowska-Powałowska, D. Use of Buckwheat Straw to Produce Ethyl Alcohol Using Ionic Liquids. *Energies* **2019**, *12*, 2014. [[CrossRef](#)]
- Hasan, A.; Rabbi, M.S.; Billah, M.M. Making the lignocellulosic fibers chemically compatible for composite: A comprehensive review. *Clean. Mater.* **2022**, *4*, 100078. [[CrossRef](#)]
- Sanjay, M.R.S.; Siengchin, S.; Parameswaranpillai, J.; Jawaid, M.; Pruncu, C.I.; Khan, A. A comprehensive review of techniques for natural fibers as reinforcement in composites: Preparation, processing and characterization. *Carbohydr. Polym.* **2019**, *207*, 108–121. [[CrossRef](#)]
- Puke, M.; Godina, D.; Kirpluks, M.; Rizikovs, J.; Brazdausks, P. Residual Birch Wood Lignocellulose after 2-Furaldehyde Production as a Potential Feedstock for Obtaining Fiber. *Polymers* **2021**, *13*, 1816. [[CrossRef](#)] [[PubMed](#)]
- Chen, H. *Biotechnology of Lignocellulose: Theory and Practice*; Chemical Industry Press: Beijing, China; Springer Science C Business Media: Dordrecht, The Netherlands, 2014. [[CrossRef](#)]
- Abbass, A.; Paiva, M.C.; Oliveira, D.V.; Lourenço, P.B.; Fangueiro, R. Insight into the effects of solvent treatment of natural fibers prior to structural composite casting: Chemical, physical and mechanical evaluation. *Fibers* **2021**, *9*, 54. [[CrossRef](#)]
- Maheswari, C.U.; Reddy, K.O.; Muzenda, E. Extraction, chemical composition, morphology and characterization of cellulose microfibrils from ficus leaves. *J. Biobased Mater. Bioenergy* **2014**, *8*, 409–414. [[CrossRef](#)]
- Liua, Y.; Lvc, X.; Baoa, J.; Xied, J.; Tanga, X.; Chea, J.; Maa, Y.; Tong, J.Y. Characterization of silane treated and untreated natural cellulosic fibre from corn stalk waste as potential reinforcement in polymer composites. *Carbohydr. Polym.* **2019**, *218*, 179–187. [[CrossRef](#)]
- Gomes, A.; Goda, K.; Ohgi, J. Effects of Alkali Treatment to Reinforcement on Tensile Properties of Curaua Fiber Green Composites. *JSME Int. J. Ser. A* **2004**, *47*, 541–546. [[CrossRef](#)]
- Alvarez, V.A.; Vazquez, A. Influence of fiber chemical modification procedure on the mechanical properties and water absorption of MaterBi-Y/sisal fiber composites. *Compos. Part A* **2006**, *37*, 1672–1680. [[CrossRef](#)]
- De Lemos, A.L. Characterization of Natural Fibers: Wood, Sugarcane and Babassu for Use in Biocomposites. *Cellul. Chem. Technol.* **2017**, *51*, 711–718.
- Poletto, M.; Ornaghi Júnior, H.L.; Zattera, A.J. Native Cellulose: Structure, Characterization and Thermal Properties. *Materials* **2014**, *7*, 6105–6119. [[CrossRef](#)] [[PubMed](#)]
- Wang, Q.; Xiao, S.; Shi, S.Q. The Effect of Hemicellulose Content on Mechanical Strength, Thermal Stability, and Water Resistance of Cellulose-rich Fiber Material from Poplar. *Bioresources* **2019**, *14*, 5288–5300. [[CrossRef](#)]
- Ando, D.; Nakatsubo, F.; Yano, H. Thermal stability of lignin in ground pulp (GP) and the effect of lignin modification on GP's thermal stability: TGA experiments with dimeric lignin model compounds and milled wood lignins. *Holzforschung* **2019**, *73*, 493–499. [[CrossRef](#)]
- Nurazzi, N.M.; Asyraf, M.R.M.; Rayung, M.; Norrrahim, M.N.F.; Shazleen, S.S.; Rani, M.S.A.; Shafi, A.R.; Aisyah, H.A.; Radzi, M.H.M.; Sabaruddin, F.A.; et al. Thermogravimetric Analysis Properties of Cellulosic Natural Fiber Polymer Composites: A Review on Influence of Chemical Treatments. *Polymers* **2021**, *13*, 2710. [[CrossRef](#)]

21. Chandrasekar, M.; Ishak, M.R.; Sapuan, S.M.; Leman, Z.; Jawaid, M. A review on the characterisation of natural fibres and their composites after alkali treatment and water absorption. *Plast. Rubber Compos.* **2017**, *46*, 119–136. [[CrossRef](#)]
22. Benini, K.C.; Mulinari, D.; Voorwald, H.; Cioffi, M.O. Chemical modification effect on the mechanical properties of hips/ coconut fiber composites. *BioResources* **2010**, *5*, 1143–1155.
23. Lee, C.H.; Khalina, A.; Lee, S.H. Importance of Interfacial Adhesion Condition on Characterization of Plant-Fiber-Reinforced Polymer Composites: A Review. *Polymers* **2021**, *13*, 438. [[CrossRef](#)]
24. Liu, C.-F.; Sun, R.-C. Chapter 5-Cellulose. In *Cereal Straw as a Resource for Sustainable, Biomaterials and Biofuels*; Sun, R.-C., Ed.; Elsevier: Amsterdam, The Netherlands, 2010; pp. 131–167. ISBN 9780444532343. [[CrossRef](#)]
25. Gupta, V.; Ramakanth, D.; Verma, C.; Maji, P.K.; Gaikwad, K.K. Isolation and characterization of cellulose nanocrystals from amla (*Phyllanthus emblica*) pomace. *Biomass Convers. Biorefinery* **2021**, 1–12. [[CrossRef](#)]
26. Boukir, A.; Fellak, S.; Doumenq, P. Structural characterization of *Argania spinosa* Moroccan wooden artifacts during natural degradation progress using infrared spectroscopy (ATR-FTIR) and X-Ray diffraction (XRD). *Heliyon* **2019**, *5*, e02477. [[CrossRef](#)] [[PubMed](#)]